Supplementary information (ESI)

Self-standing polyaniline membrane containing quaternary ammonium groups loaded with hollow spherical $NiCo_2O_4$ electro-catalyst for alkaline water electrolyser

Mani Bhushan,[ab] Mariappan Mani, [bc] Anuj K. Singh,[ab] Asit B. Panda,[bc] and Vinod K. Shahi,*[ab]

ESI S1. The FT-ATR technique with spectrum GX series 49387 spectrometer in the range of 4000–400 cm^{-1} was used for FTIR spectra.

Scanning electron microscopy (SEM) was recorded by Leo microscope (Kowloon, Hong Kong) after gold sputter coatings on dried membrane samples. SEM analysis was performed with dried membrane samples (OH^- form) using SEM LEO 1430 VP instrument at 10 kV.

Transmission electron microscope (TEM) images were collected using a JEOL JEM 2100 microscope (TEM).

A Philips X'pert X-ray powder diffractometer was used to record XRD patterns.

The surface area and pore size was obtained using an ASAP 2010 micrometrics, USA, surface area analyser.

ESI S2. Thermo-gravimetric analyzer (NETZSCH TG 209F1 Libra TGA209F1D-0105-L) was used for the analysis of membranes thermal stability under a nitrogen atmosphere with a heating rate of 10 °C/min from 30 to 700 °C.

Differential scanning calorimetry (DSC) measurements were performed between 30-350 °C with 5 °C/min heating rate using Mettler Toledo DSC822e thermal analyzer with Stare software.

The dynamic mechanical stability of the composite membranes was evaluated by using a dynamic mechanical analyzer (Mettler Toledo; DMA) 861c instrument with starc software under a nitrogen atmosphere with a heating rate of 10 °C/min from 30 to 250 °C.

ESI S3. The water uptake (WU) of membrane samples was measured in OH^- form. The surface water of the wet membrane samples (soaked in deionized water for 24 hrs) was sponged with tissue paper and weight of wet membrane (W_{wet}) was recorded. Further, membrane sample was dried in vacuum oven (80 ^oC for 12 h) and weight of dry membrane (W_{dry}) was obtained. WU values was estimated by percentage weight difference.

Membrane swelling ratio was obtained from dimensional differences between wet at dry samples.

$$Swelling\ ratio = \frac{L_{wet} - L_{dry}}{L_{dry}} \times 100 \qquad (1)$$

Average size of wet and dry membrane (L_{wet} and L_{dry}, respectively) may be defined as $L_{wet} = (L_{wet1}\ L_{wet2})^{1/2}$ and $L_{dry} = (L_{dry1}\ L_{dry2})^{1/2}$

Ion exchange capacity (IEC) defines the moles of ionic moiety present per unit mass of the dry membrane, was measured by classical acid-base titration method. Vacuum dried membrane) of known weight (W_{dry}) was equilibrated in NaOH (0.10 M) solution for 24 h and exchanged OH- was back titrated with standardized HCl solution using phenolphthalein as indicator, IEC was calculated using the following equation.:

$$IEC = \frac{C_{HCl}\ V_{HCl} - C_{NaOH}\ V_{NaOH}}{W_{dry}} \qquad (2)$$

Where C and *V* denote the concentration and volume of HCl or NaOH.

Measurement of transport number (t+): Electrical potential that developed when ion exchange separating the two electrolyte solution of different concentration is known as membrane potential

(E_m). The value of developed potential depends on membrane intrinsic property and electrolyte concentrations. The membrane potential was measured with exposing 8 cm^2 membrane area between two compartment cell with continuous flowing of 0.1 M and 0.01 M KOH solution. The developed potential across the membrane was measured using multimeter (FLUKE 15B +) connected with saturated calomel electrode reference electrode. The transport number (t_-) calculated by using the given formula:

$$E\mathrm{m} = \frac{RT(2t_- - 1)}{F} ln \frac{C1}{C2} \qquad (3)$$

Where R is the gas constant, F is the Faraday constant, T is the absolute temperature (298 °K), C_1 and C_2 are the concentration of electrolyte solutions in the two compartment..

In-plane proton conductivity of studied membrane samples was measured using four-electrode AC impedance potentiostat/galvanostat frequency response analyzer (Eco Chemie, B.V. Utrecht, The Netherlands Auto Lab, model PGSTAT 302N) over 1-10^6 Hz frequency range. The membrane sample in OH^- form was mounted between two in-house made stainless steel circular electrodes. Direct current (dc) and sinusoidal alternating currents (ac) were supplied to the respective electrodes for recording the frequency at 1 μA/s scanning rate. The membrane resistance (R^m; Ω) was calculated by Nyquist plots using Fit and Simulation method, and membrane conductivity (κ^m, S cm^{-1}) was estimated by the following equation,

$$\kappa^m = L \Big/ R^m A \qquad (4)$$

Where L (cm) and A (cm^2) are the membrane thickness and membrane conducting area, respectively.

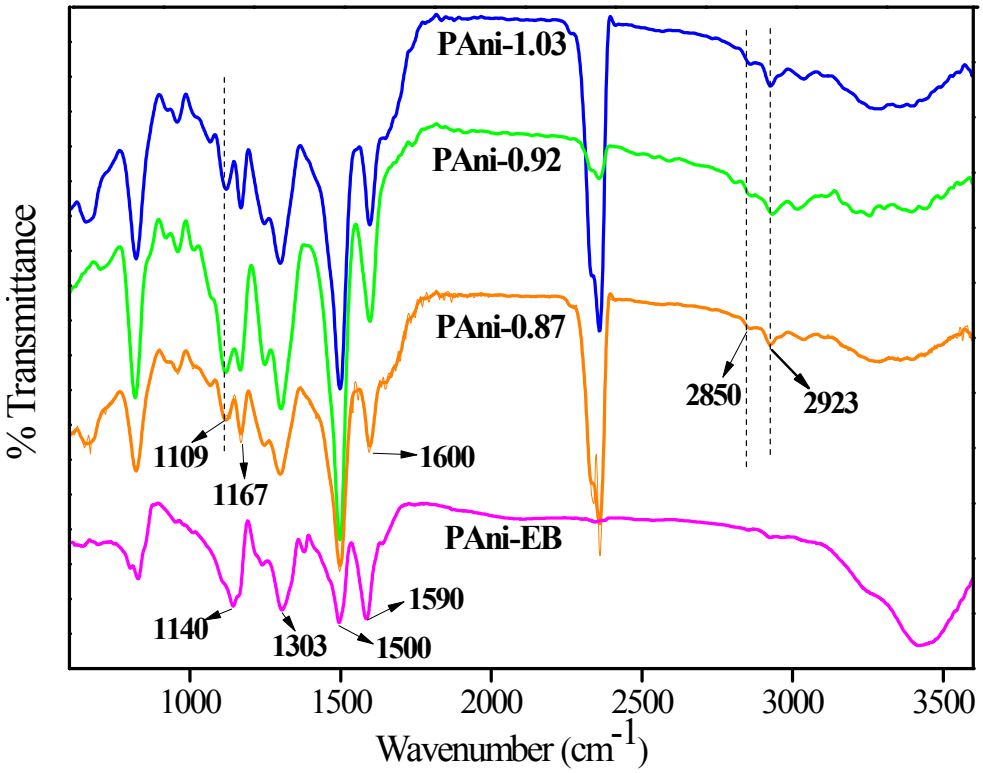

Fig. S1. FT-ATR IR spectra of prepared PAni-EB powder, PAni-0.87, PAni-0.92 and PAni-1.03 membranes.

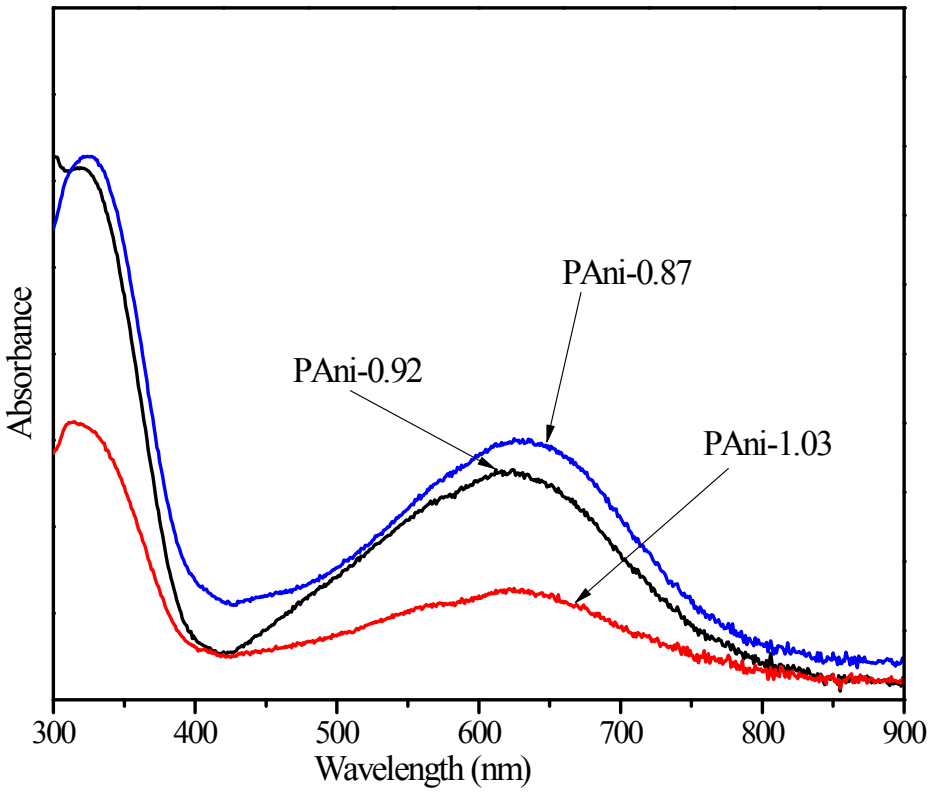

Fig. S2. UV-Vis spectra of PAni-0.87, PAni-0.92 and PAni-1.03 membrane casting solutions.

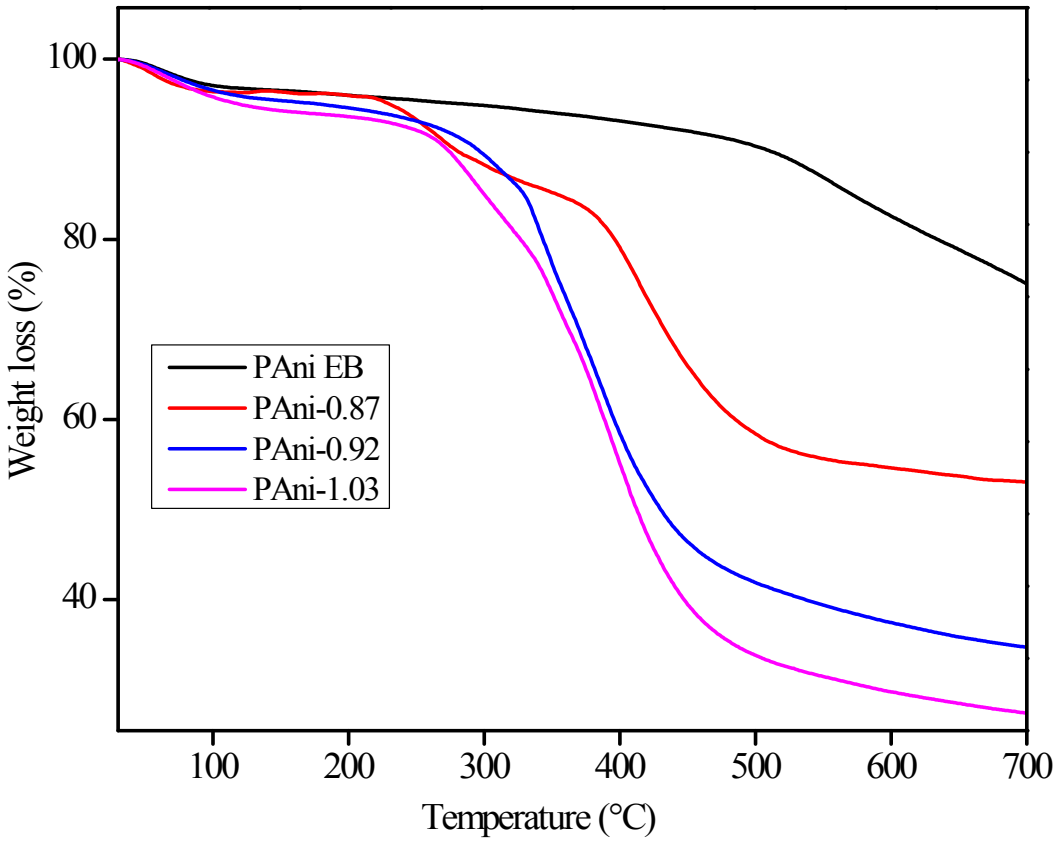

Fig. S3. TGA curves for PAni-EB powder, PAni-0.87, PAni-0.92 and PAni-1.03 membranes.

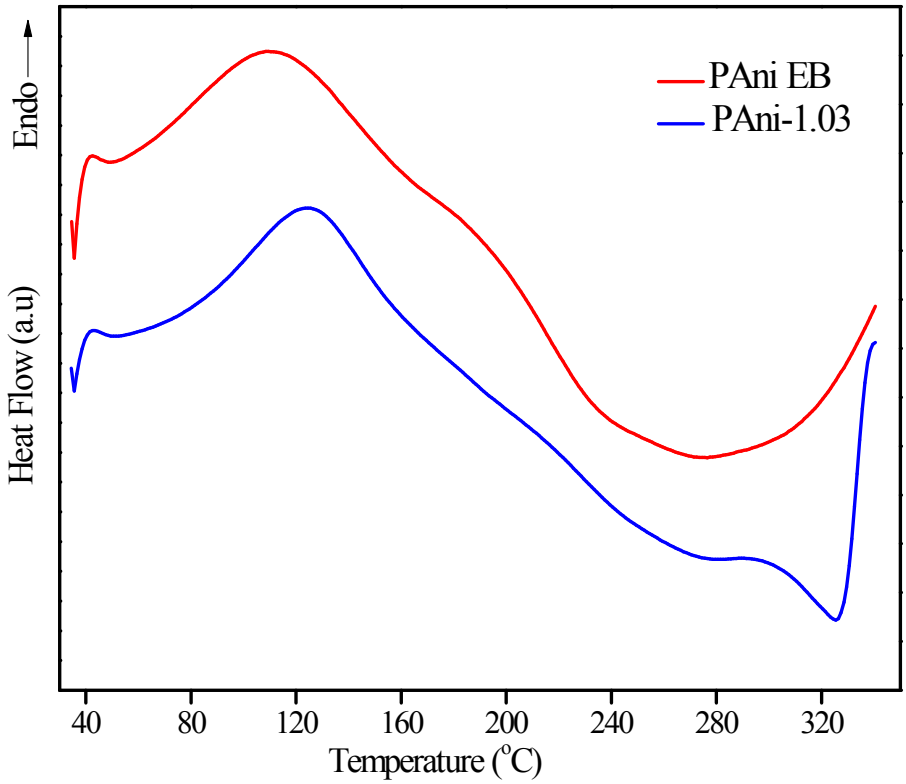

Fig. S4a. DSC analysis of PAni-EB powder and PAni-1.03 membrane.

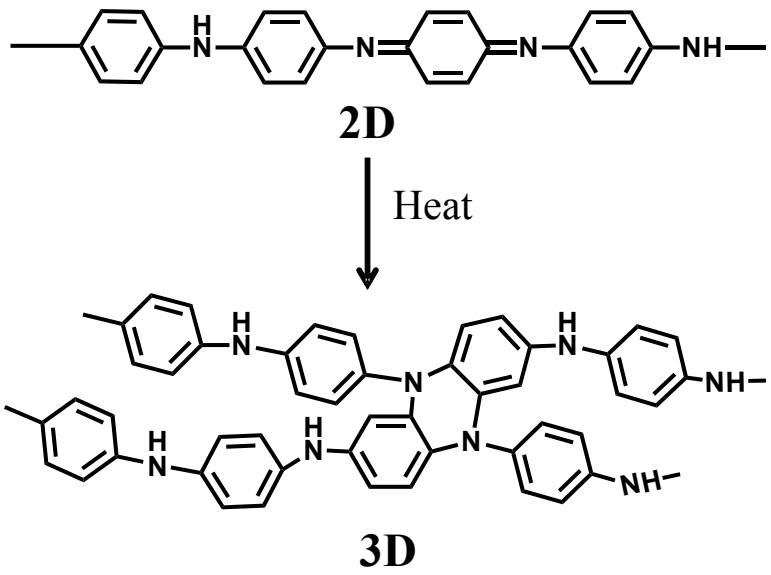

Fig. S4b. Thermal crosslinking between PAni-EB matrixes.

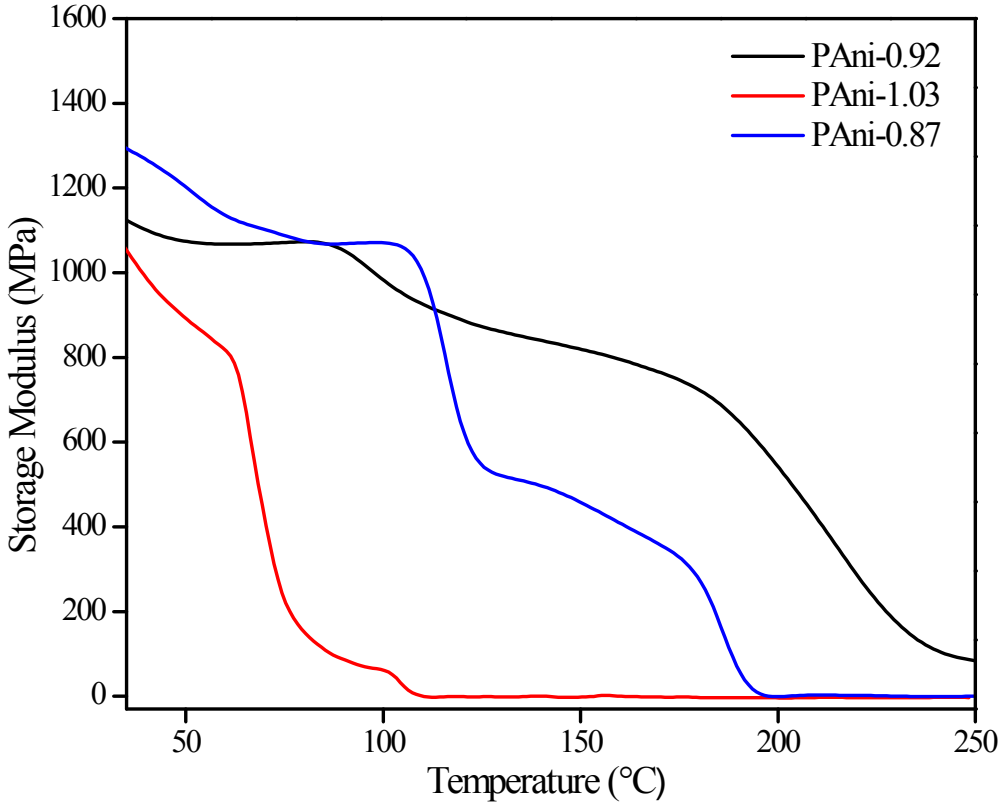

Fig. S5. DMA curves for PAni-1.03, PAni-0.92 and PAni-0.87 membranes.

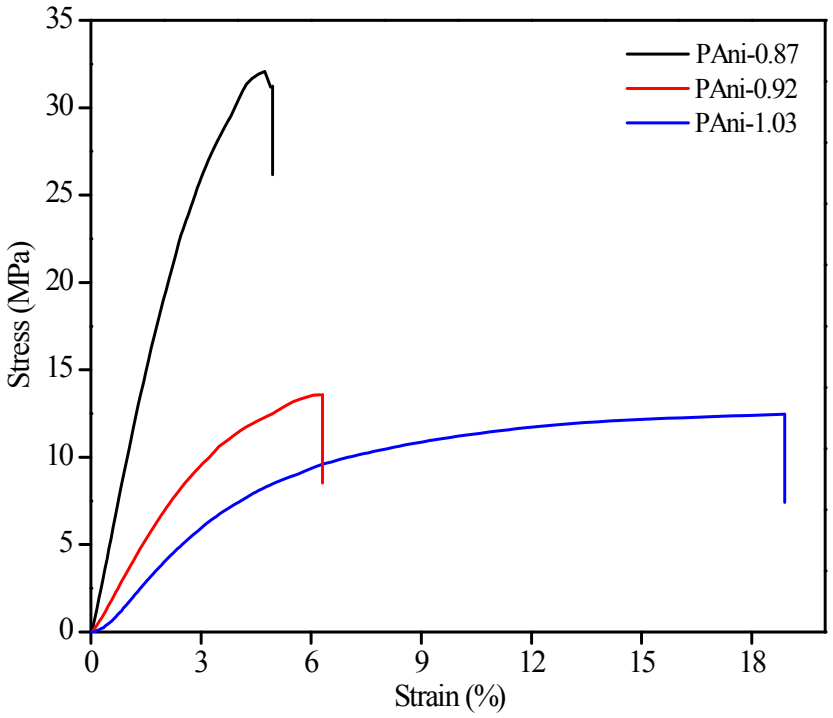

Fig. S6. Stress-strain curves for PAni-0.87, PAni-0.92 and PAni-1.03 membranes.

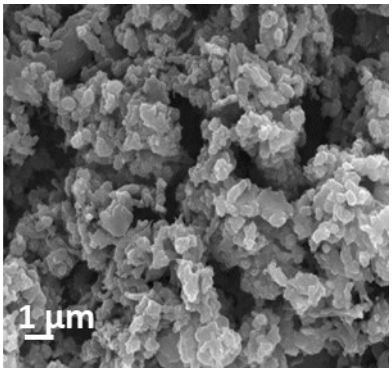

Fig. S7. The SEM image of PAni-EB powder.

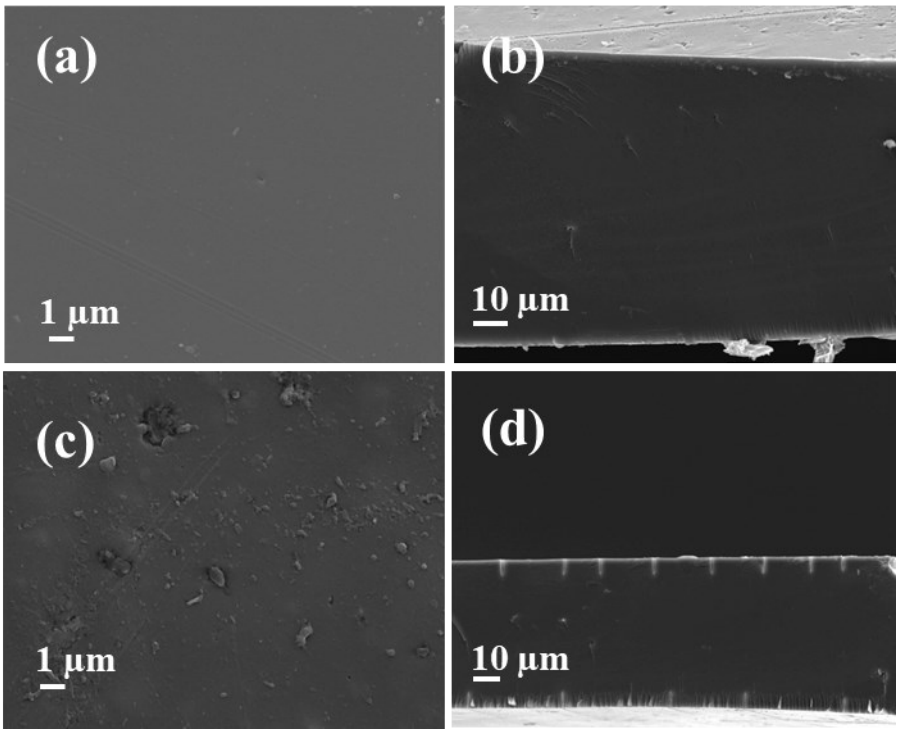

Fig. S8. SEM images (a, c) surface and (b, d) cross-section of PAni-1.03 membrane before and after treatment with 1.0 M KOH at 80 °C for 48 hrs.

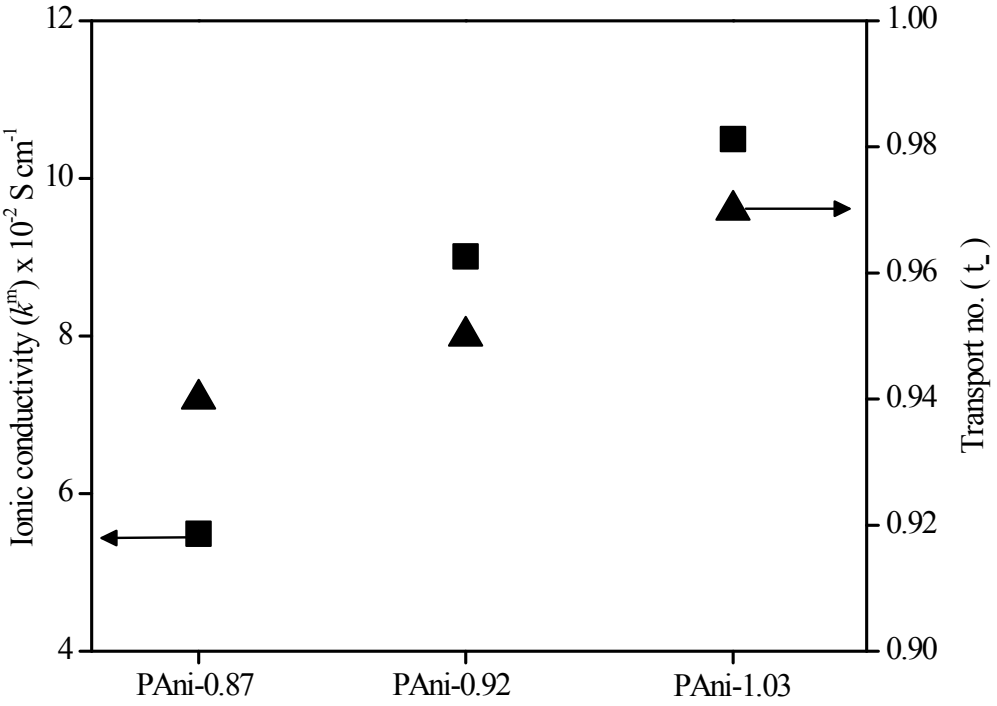

Fig. S9. Ionic conductivity *vs* counter-ion transport number (t_-) values for different PAni-X AEMs.

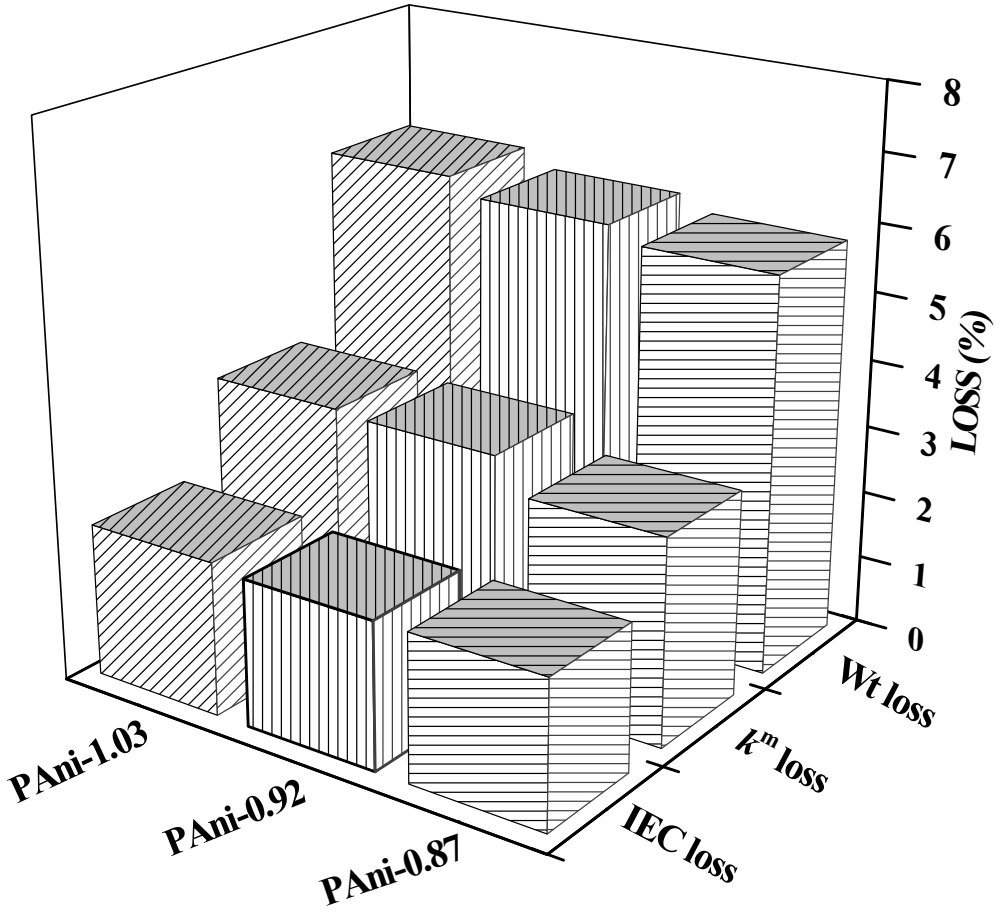

Fig. S10. Loss (%) in weight, ionic conductivity and IEC of different PAni-X AEMs after treatment with 1.0 M KOH at 80 °C for 48 hrs.

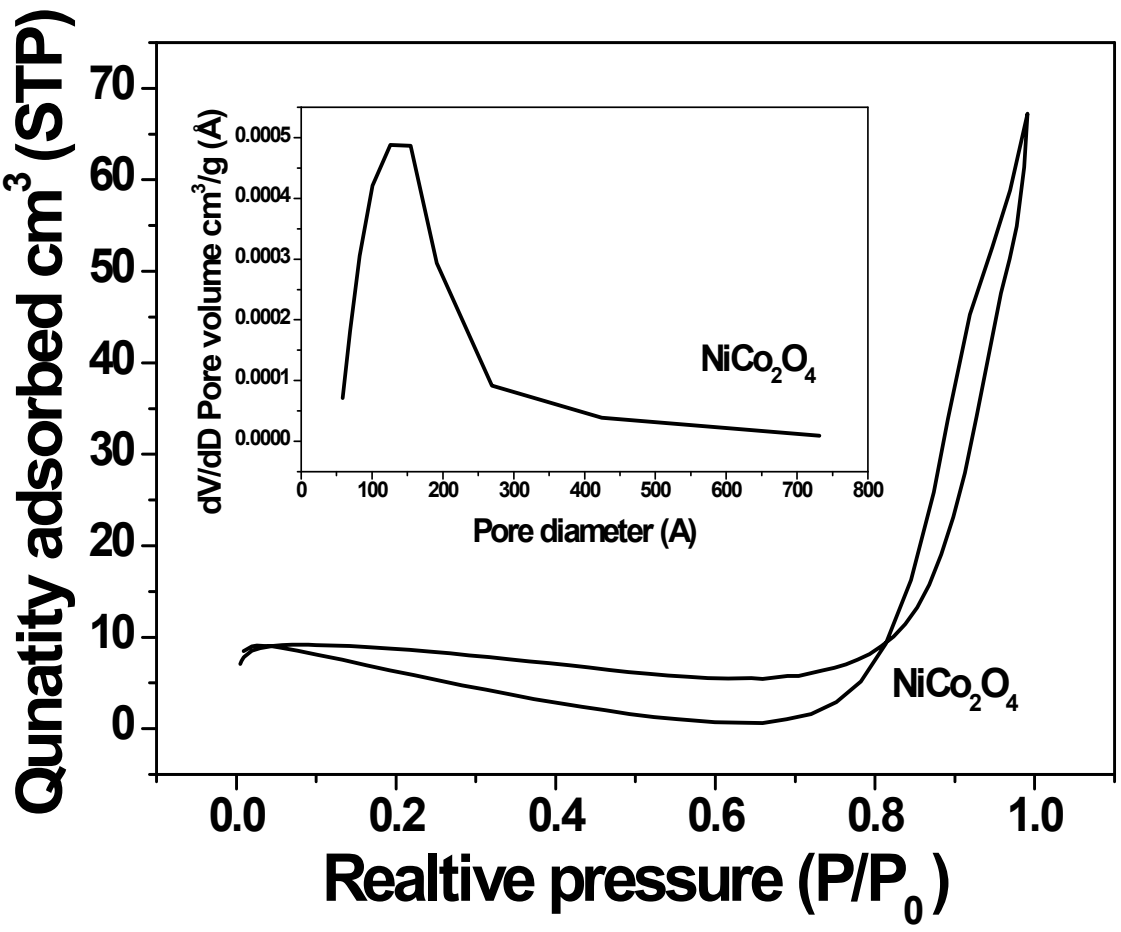

Fig. S11. N_2 sorption isotherms and corresponding pore size distribution (inset) curve of the synthesized samples.

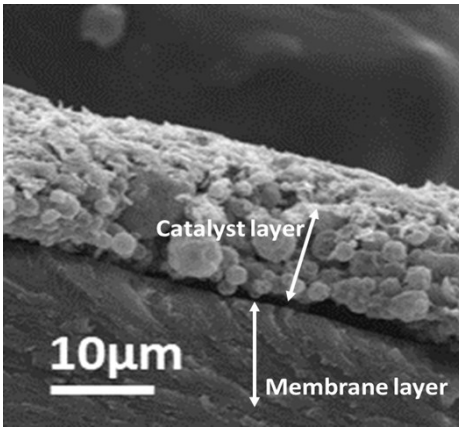

Fig. S12. Magnified FE-SEM cross-section image after catalyst loading on PAni-1.03 membrane.

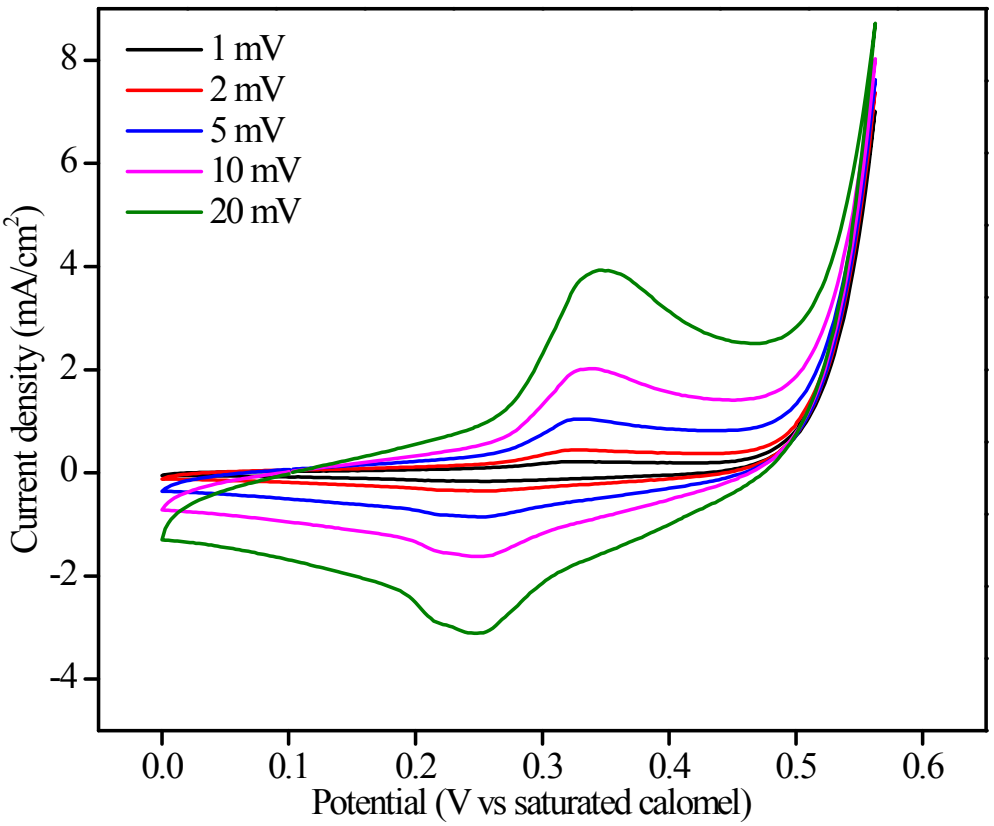

Fig. S13. Cyclic Voltammetry of catalyst at different scan rates in 1.0 M KOH.

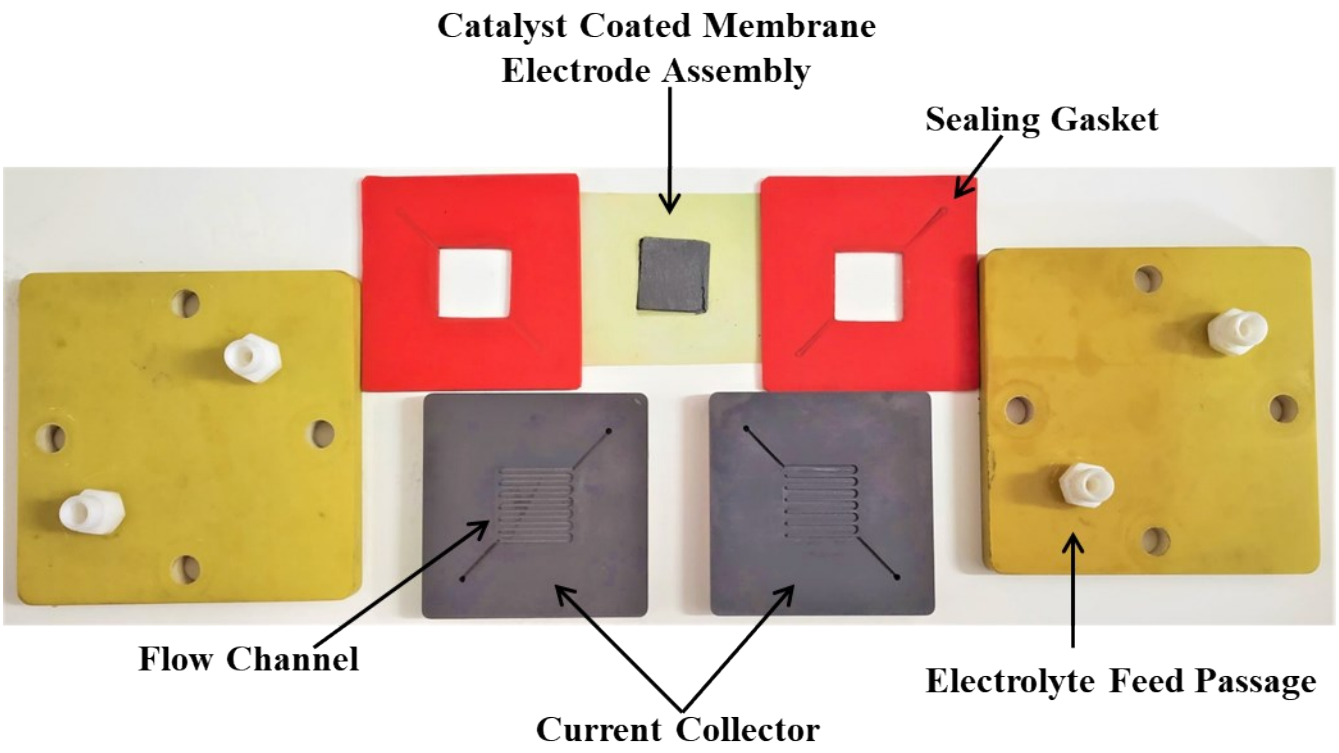

Fig. S14. Optical images of different components used for assembly of alkaline water electrolyzer.

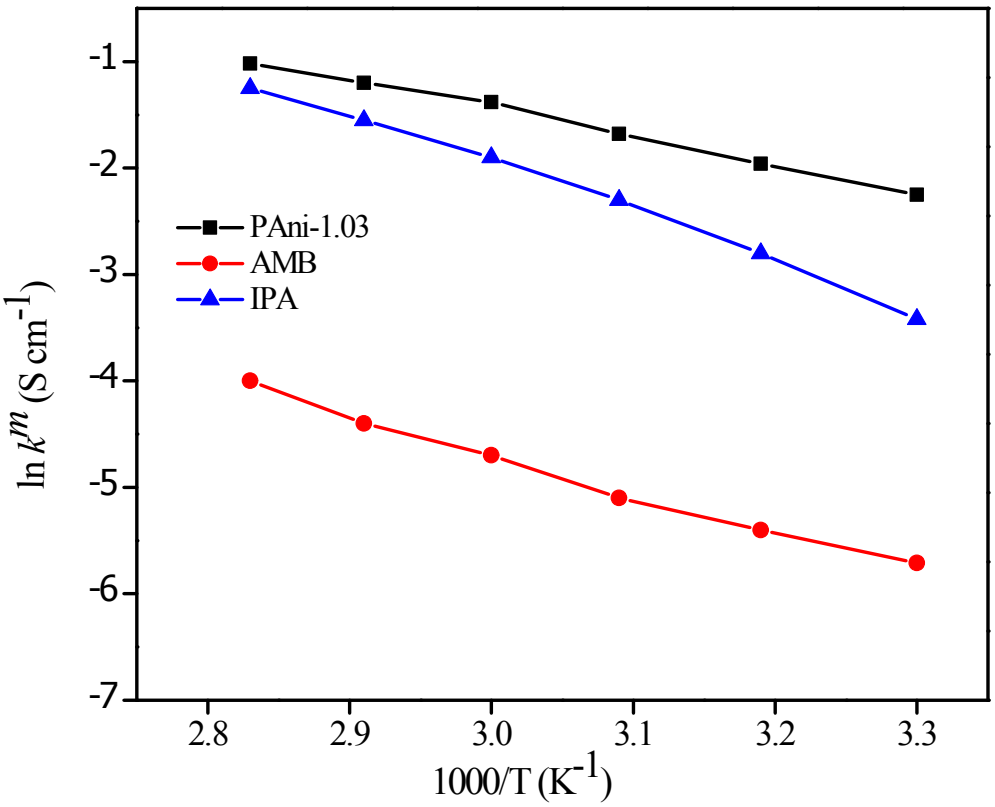

Fig. S15. Arrhenius plots for PAni-1.03, AMB and IPA membranes.

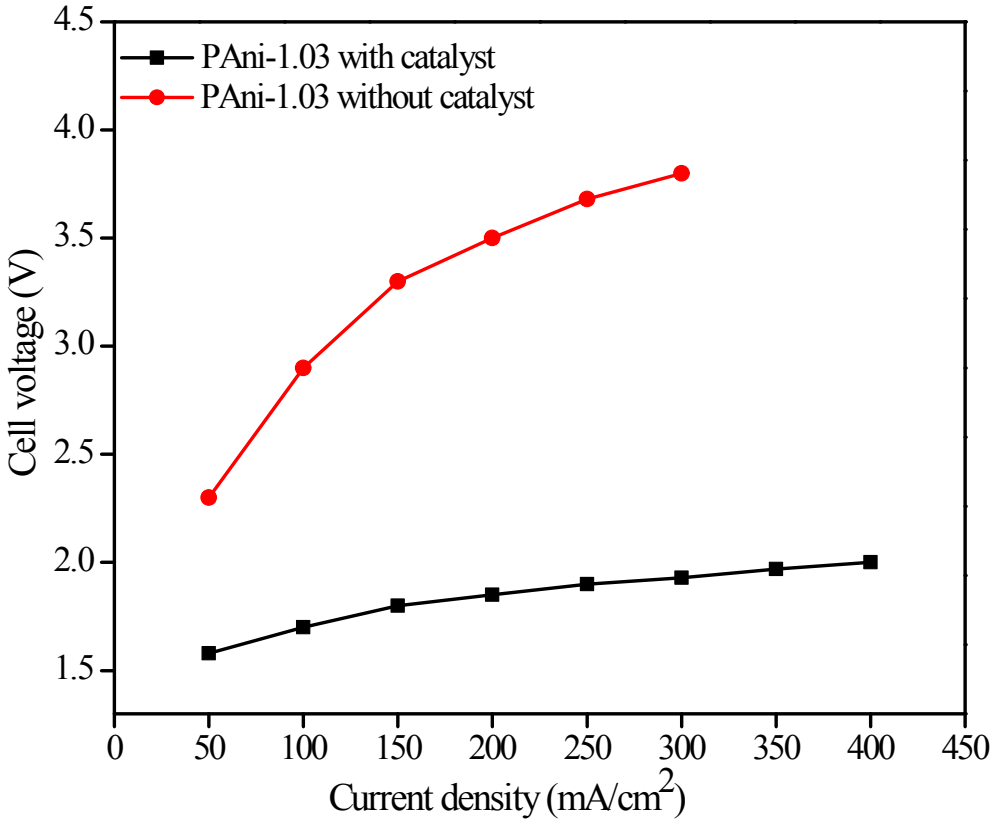

Fig. S16. Water electrolysis performance of PAni-1.03 AEM with and without catalyst